

## EVALUATION OF TOPOLOGICAL FORMS FOR WEIGHT-EFFECTIVE OPTIMUM DESIGN OF SINGLE-SPAN STEEL TRUSS BRIDGES

O. Hasaebi\*<sup>a</sup> and E. Dođan<sup>b</sup>

<sup>a</sup> Department of Civil Engineering, Middle East Technical University, Ankara, Turkey

<sup>b</sup> Department of Engineering Sciences, Middle East Technical University, Ankara, Turkey

**Received:** 5 December 2010, **Accepted:** 25 January 2011

### ABSTRACT

This paper reports a comparative study on design weight efficiency of single span steel truss bridge topologies subjected to gravity loads. The bridges configured according to nine distinct topological forms (namely, Pratt, Parker, Baltimore, Petit, K-Truss, Warren, Subdivided Warren, Quadrangular Warren and Whipple) are designed for minimum weight under various span length requirements of single span truss bridges, and the results obtained with these topological forms are compared. The optimization process for each bridge topological form requires achieving optimal sizing of members as well as determining coordinates of the top chord nodes such that the least design weight is attained for the bridge. The design constraints and limitations are imposed according to serviceability and strength provisions of ASD-AISC (Allowable Stress Design Code of American Institute of Steel Institution) specification. The optimization algorithm employed is based on simulated annealing method.

**Keywords:** Structural optimization; single-span steel truss bridges; bridge topological forms; minimum weight design; design weight efficiency; simulated annealing

### 1. INTRODUCTION

Over the years steel truss bridges have kept their popularity amongst bridge engineers, not only because these systems offer certain advantages from structural and constructional standpoints, but also they enable an opportunity to build up large span bridges with relatively less amount of material. Single span steel truss bridges refer to a subset of these systems where the entire opening is crossed with a single bridge span with generally simply supported end conditions. Especially, they are preferable in cases where the disturbance to the stream bed needs to be avoided.

The single span truss bridges can be designed in a variety of different topological forms,

---

\* E-mail address of the corresponding author: oguzhan@metu.edu.tr (O. Hasaebi)

such as Pratt, Parker, Baltimore, Petit, K-Truss, Warren, Subdivided Warren, Quadrangular Warren, Whipple, etc. The Pratt truss has a topological feature such that the diagonals are all sloped in the same direction on each side of the truss around the mid-span. In this form of truss bridge, the upper chord and vertical members are subjected to compression whereas the diagonals and lower chord members are under tension. The Baltimore truss has additional bracing members in the lower section to prevent buckling in the compression members as well as to control deflection. Both Pratt and Baltimore trusses have a constant height throughout the span length of the bridge. The Parker and Petit trusses have identical topological forms with Pratt and Baltimore trusses, respectively, except that the formers have a polygonal shape with the bridge height increasing from the ends towards the mid-span. In the Warren truss alternate diagonals sloped in different directions frame into each others at lower chord nodes. The Subdivided Warren truss has the topological form of Warren truss with vertical members having sub-diagonals and sub-verticals. The Quadrangular Warren is a double intersection truss form with alternating tension and compression diagonals. The K-truss is configured in the form of letter “K” by the orientation of the vertical member and two oblique members in each panel. Finally, the Whipple truss is the one having elongated and usually thin tension members which cross two or more members.

This study is concerned with evaluation and comparison of weight efficiency of these nine topological forms under different span length requirements (100, 200, 400 and 600 ft) of single span steel truss bridges. The bridges that are subjected to gravity loads are first configured according to these topological forms, and the resulting structures are optimized for minimum design weight subject to strength, stability and displacements provisions of ASD-AISC [1]. In the optimum design process, both size (discrete) and shape (continuous) design variables are employed together and simultaneously. In this context, size variables are used to choose appropriate sizes for the bridge members, whereas the optimal height and/or shape of the bridge’ upper chord are searched with shape variables [2]. The optimization routine used in the study is based on simulated annealing algorithm developed in Bennage and Dhingra [3]. This algorithm employs a numerical optimization procedure that mimics annealing process in thermodynamics applied for bringing the physical systems to their minimum energy levels.

## 2. OPTIMUM DESIGN PROBLEM FORMULATION

Optimum design of a single-span truss bridge requires the selection of structural members from a standard steel section table and determining the height or shape of the upper chord of the bridge such that the bridge satisfies the strength and serviceability requirements imposed by a code of practice, while the minimum weight of the bridge is attained. Accordingly, the objective function ( $W$ ) can mathematically be defined as follows:

$$W = \sum_{m=1}^{N_m} \rho_m L_m A_m \quad (1)$$

The problem constraints can be formulated as follows:

$$g_m = \frac{\sigma_m}{(\sigma_m)_{all}} - 1 \leq 0 \quad \text{and} \quad s_m = \frac{\lambda_m}{(\lambda_m)_{all}} - 1 \leq 0, \quad m = 1, \dots, N_m \quad (2)$$

$$\delta_{j,k} = \frac{d_{j,k}}{(d_{j,k})_{all}} - 1 \leq 0, \quad j = 1, \dots, N_j \quad (3)$$

In Eqs. (1-3),  $A_m$ ,  $L_m$  and  $\rho_m$  represent the cross-sectional area, length and unit weight of the  $m$ -th member of the bridge, respectively;  $N_m$  and  $N_j$  are the total number of members and joints in the bridge, respectively;  $g_m$ ,  $s_m$  and  $\delta_{j,k}$  are referred to as constraints being bounds on stresses, slenderness ratios and displacements, respectively;  $\sigma_m$  and  $(\sigma_m)_{all}$  are the computed and allowable axial stresses for the  $m$ -th truss member, respectively;  $\lambda_m$  and  $(\lambda_m)_{all}$  are the slenderness ratio and its upper limit for  $m$ -th member, respectively; finally  $d_{j,k}$  and  $(d_{j,k})_{all}$  are the displacements computed in the  $k$ -th direction of joint  $j$  and its permissible value, respectively.

In the present study, all the strength and serviceability limitations are imposed as to ASD-AISC [1] specification, and the integration of these constraints with the objective function is implemented using a penalty function approach, which is discussed in detail in Hasançebi et al. [4].

### 3. SIMULATED ANNEALING

Simulated annealing (SA) searches for minimum energy states using an analogy based upon the physical annealing process. In this process, a solid initially at a high energy level is cooled down gradually to reach its minimum energy and thus to regain proper crystal structure with perfect lattices. The idea that this process can be simulated to solve optimization problems is made possible by establishing a direct analogy between minimizing energy level of a physical system and lowering cost of an objective function [5]. The successful applications of the method in the fields of structural optimization and computational structural mechanics have been reported in a number of publications in the literature, such as Refs. [6-9]. In Hasançebi et al. [10], a reformulation of SA algorithm is presented, resulting in significant performance improvement of the technique for large-scale optimization problems. The basic computational steps of a standard SA algorithm are outlined in the following.

Step 1: The first step is the setting of an appropriate cooling schedule. After choosing suitable values for starting acceptance probability ( $P_s$ ), final acceptance probability ( $P_f$ ), and the number of cooling cycles ( $N_c$ ), the cooling schedule parameters are calculated as follows:

$$T_s = -\frac{1}{\ln(P_s)}, \quad T_f = -\frac{1}{\ln(P_f)}, \quad \eta = \left[ \frac{\ln(P_s)}{\ln(P_f)} \right]^{1/N_c - 1} \quad (4)$$

In Eq. (4),  $T_s$ ,  $T_f$  and  $\eta$  are referred to as starting temperature, final temperature, and the cooling factor, respectively. The starting temperature is assigned as the current temperature, i.e.,  $T = T_s$ .

Step 2: The next step is to originate an initial design via random initialization. This design is assigned as the current solution of the optimization process and its objective function ( $\phi_c$ ) is calculated.

Step 3: A number of candidate designs are generated in the close vicinity of the current design. This is performed as follows: (i) a design variable ( $I_i$ ) is selected, (ii) this variable is given a small perturbation ( $z_i$ ) in a predefined neighborhood (Eq. 5) and (iii) finally, a candidate design is generated by assuming the perturbed value ( $I'_i$ ) of the variable, while keeping all others same as in the current design. Each design variable is selected only once in a random order to yield a candidate design.

$$I'_i = I_i \pm z_i \quad (5)$$

Step 4: Each time when a candidate design is generated, its objective function value ( $\phi_a$ ) is first computed and then it is set to compete with the current one. If the candidate provides a better solution, it is accepted automatically and it replaces the current design. If not, the so-called Metropolis test is applied to determine the winner, in which case the probability of accepting a poor candidate ( $P$ ) is assigned as follows:

$$P = \exp(-\Delta\phi / KT) \quad (6)$$

where  $T$  is the current temperature of the process and  $K$  is the Boltzman parameter which is manipulated as the working average of  $\Delta\phi$  values.

Step 5: A single iteration of a cooling cycle is referred to the case where all design variables are selected once and perturbed to generate candidate designs. A cooling cycle is iterated a certain number of times in the same manner to ensure that objective function is reduced to a reasonably low value within the cycle.

Step 6: After the cooling cycle is iterated a number of times, the temperature is reduced by the ratio of the cooling factor  $\eta$ , and the temperature of the next cooling cycle is set as in Eq. (7), where  $T^k$  and  $T^{k+1}$  denote the temperature at the  $k$  and  $(k+1)$ -th cooling cycles, respectively.

$$T^{k+1} = T^k \eta \quad (7)$$

#### 4. DESIGN EXAMPLES

The design examples are carried out to numerically investigate economical span lengths of the truss bridge topologies. Taking into account the fact that the majority of single span bridges built in practice are amongst 100-600 ft (30.5-183.0 m) long, four different span lengths ( $L$ ), namely 100, 200, 400 and 600 ft are considered as separate case studies, Figure 1. For each of these span lengths, nine bridge models are generated by configuring the

structural system according to the nine aforementioned topological forms adopted for single-span steel truss bridges. For each model, the panel points are spaced equally through the span and are set to a constant value of 25 ft (7.62 m). The design loads are determined according to the provisions of ASCE 7-05[11]. Live loads that result from traffic are combined together with dead loads of the deck and floor systems, which are later on transmitted to the lower chord, resulting in equivalent panel point loads of 60kips (267kN) at each node in any model.

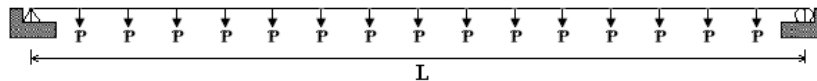


Figure 1. Truss bridge design problem.

In the optimum design process both size and shape design variables are employed together. Size variables are used to determine the required steel sections for bridge members and are grouped considering the symmetry of the structures. They are selected from a total of 83 wide-flange sections ranging between W10x12 and W14x730. The shape variables are chosen to determine the height and/or shape of the upper chord of a bridge model, again considering a desired symmetry of the structure about mid-span. The number of shape variables used in a model depends on the bridge topological form. For example, a single shape variable is used to define the height in bridge models with Pratt, Baltimore, Warren, Subdivided Warren, Quadrangular Warren, Whipple and K-truss forms, since they have a straight upper chord. In Parker and Petit forms, however, the y-coordinates of all upper chord nodes are allowed to vary. The ranges of shape variables are chosen between zero and half of the span length ( $L/2$ ). In all the bridge models, the strength and stability requirements of the designs are specified in accordance with ASD-AISC [11] provisions. Besides, the maximum displacements of panel points in any direction are restricted to  $1/600$  of the total span length. The following material properties of the steel are used:  $F_y$  (yield stress) = 36 ksi ( $2531 \text{ kg/cm}^2$ ) and  $E$  (modulus of elasticity) = 29,000 ksi ( $2,038,936 \text{ kg/cm}^2$ ).

The optimum design for each model is sought by running the solution algorithm five times independently due to stochastic nature of the SA technique. The maximum computing time for a single run of a test problem is recorded as 12 min on a serial computer with Intel Quad Core Q9300 2.5GHZ LGA775 processor.

#### 4.1 Case 1: 100ft long span bridge

In the first case study, the span length is set to 100ft. The lower chord of the bridge consists of four equal panels, and it has three panel point loads acting on each node. It is intended to generate nine bridge models for this span length by choosing bridge topologies according to Pratt, Parker, Baltimore, Petit, K-Truss, Warren, Subdivided Warren, Quadrangular Warren and Whipple forms. However, as shown in Figure 2, it is found that only four of them namely, Parker, K-Truss, Quadrangular Warren and Warren are applicable to this case; the other topological forms cannot be generated due to presence of inadequate number of panels. The bridge models employed have 7, 9, 8 and 7 size variables, respectively. Parker truss, whose upper chord nodes are allowed to vary, has two and the others have only one shape variable.

The best (optimum) designs obtained for the bridge under four different topological forms are tabulated in Table 1 with section designations attained for each member group and the resulting values of shape variables in conjunction with design variable numbering shown in Figure 2 for each model.

Table 1: Optimum designs obtained for 100ft long span bridge under various topological forms.

Variable	Bridge topological forms								
	Pratt	Parker	Baltimore	Petit	K_truss	Warren	Q_Warren	S_Warren	Whipple
<i>Size variables, ready sections</i>									
$A_1$	N/A	W10x22	N/A	N/A	W10x22	W10x22	W10x22	N/A	N/A
$A_2$	N/A	W10x22	N/A	N/A	W10x22	W10x22	W10x22	N/A	N/A
$A_3$	N/A	W12x65	N/A	N/A	W10x12	W12x65	W12x65	N/A	N/A
$A_4$	N/A	W10x12	N/A	N/A	W10x22	W10x12	W10x12	N/A	N/A
$A_5$	N/A	W10x22	N/A	N/A	W12x65	W10x22	W10x22	N/A	N/A
$A_6$	N/A	W10x49	N/A	N/A	W10x15	W10x54	W10x22	N/A	N/A
$A_7$	N/A	W10x17	N/A	N/A	W10x33	W10x12	W10x54	N/A	N/A
$A_8$	N/A	N/A	N/A	N/A	W10x49	N/A	W10x22	N/A	N/A
$A_9$	N/A	N/A	N/A	N/A	W10x12	N/A	N/A	N/A	N/A
<i>Shape variables (in.)</i>									
$y_1$	N/A	195	N/A	N/A	209	217	221	N/A	N/A
$y_2$	N/A	246	N/A	N/A	N/A	N/A	N/A	N/A	N/A
Weight,lb (kg)	-	10611.83 (4814.80)	-	-	12202.24 (5536.41)	10919.70 (4954.49)	12516.32 (5678.91)	-	-

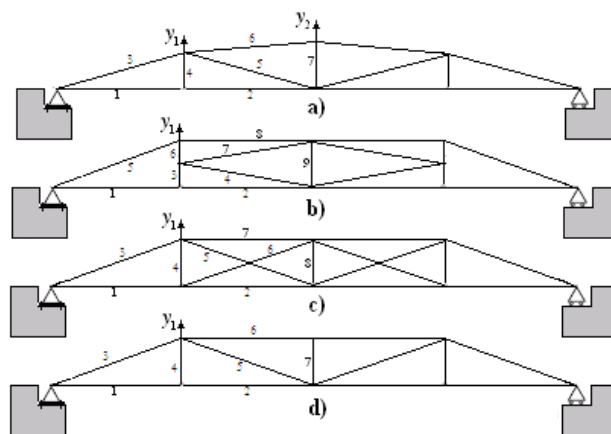


Figure 2. The topological forms used to configure 100 ft long span bridge: a) Parker, b) K-truss, c) Quadrangular Warren, d) Warren

The minimum weight design for the bridge is produced by Parker truss with a design weight of 10,611.83 lb (4,813.52 kg). This design is followed by Warren truss with the corresponding design weight of 10919.70 lb (4,953.17 kg). Quadrangular Warren truss produces the heaviest bridge with a design weight of 12,516.32 lb (5,677.39 kg). The design history curve representing the variation of the best feasible obtained thus far in the optimum design process is plotted in Figure 3 for each bridge model.

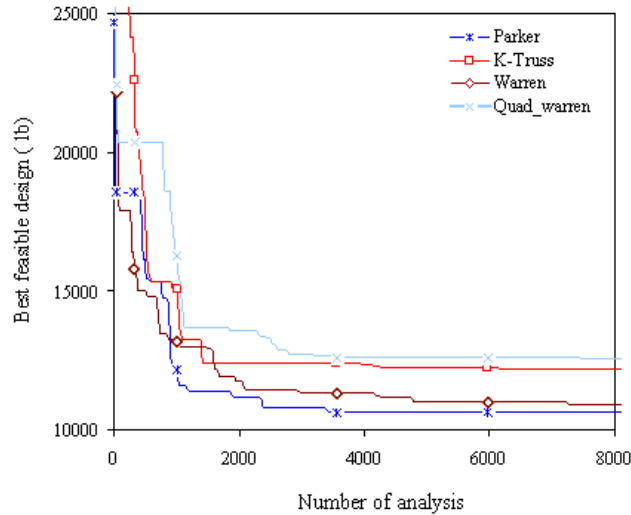


Figure 3. The design history curve of the best solution recorded under each topological form for 100ft long span bridge

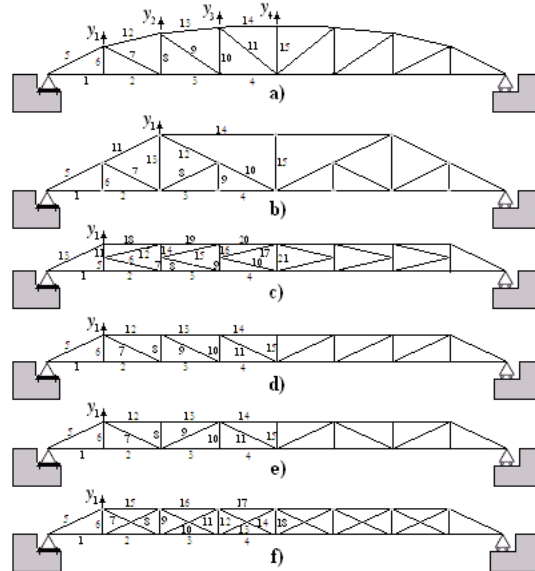


Figure 4. The topological forms used to configure 200 ft long span bridge: a) Parker, b) Baltimore, c) K-truss, d) Pratt, e) Warren, f) Quadrangular Warren

#### 4.2 Case 2: 200ft long span bridge

In this case study, the span length has increased to 200 ft. Eight panels are equally spaced in the lower chord of the bridge, which has seven panel point loads acting on each node. Again some topological forms, namely Baltimore, Petit and Whipple are not applicable to this case due to small number of panels. Hence, six bridge forms (Pratt, Parker, K- truss, Warren, Quadrangular Warren and Subdivided Warren) are employed with 15, 15, 21, 15, 18 and 15 size design variables, respectively. The geometry and member grouping of the bridge models are displayed in Figure 4. Except for Parker truss, which has four shape variables, all other bridge forms incorporate a single shape variable. The best (optimum) designs obtained for the bridge under six different topological forms are tabulated in Table 2. It is again noticed that with a design weight of 40,777.72 lb (18,493.29 kg), Parker truss form yields the best design for 200ft long span bridge. This design is followed by K-truss, having a weight of 47,158.78 lb (21,386.85 kg). The most uneconomical solutions are produced by Pratt and Quadrangular Warren trusses with design weights of 54,052.20 lb (24,513.47 kg) and 58,215.70 lb (26,401.68 kg), respectively. Figure 5 shows the design history curves for the best solution of each model.

Table 2: Optimum designs obtained for 200ft long span bridge under various topological forms.

Variable	Bridge topological forms								
	Pratt	Parker	Baltimore	Petit	K_truss	Warren	Q_Warren	S_Warren	Whipple
<i>Size variables, ready sections</i>									
$A_1$	W10x39	W14x38	N/A	N/A	W14x30	W14x38	W10x33	W14x38	N/A
$A_2$	W12x35	W14x38	N/A	N/A	W14x34	W10x26	W12x40	W10x39	N/A
$A_3$	W14x82	W10x45	N/A	N/A	W12x65	W14x82	W12x79	W14x38	N/A
$A_4$	W12x87	W14x48	N/A	N/A	W10x68	W10x68	W10x68	W14x38	N/A
$A_5$	W14x109	W14x99	N/A	N/A	W10x12	W14x109	W14x109	W14x99	N/A
$A_6$	W10x22	W10x19	N/A	N/A	W10x30	W10x22	W12x26	W10x19	N/A
$A_7$	W12x53	W10x22	N/A	N/A	W10x22	W10x49	W10x33	W10x45	N/A
$A_8$	W12x53	W10x22	N/A	N/A	W10x22	W10x22	W10x49	W10x45	N/A
$A_9$	W12x40	W10x33	N/A	N/A	W10x12	W12x72	W10x22	W10x19	N/A
$A_{10}$	W10x39	W12x26	N/A	N/A	W10x22	W10x22	W10x54	W10x22	N/A
$A_{11}$	W10x33	W10x33	N/A	N/A	W14x34	W10x33	W10x33	W14x90	N/A
$A_{12}$	W12x79	W12x87	N/A	N/A	W10x60	W12x72	W10x22	W10x22	N/A
$A_{13}$	W14x99	W12x87	N/A	N/A	W14x109	W12x87	W10x49	W10x33	N/A
$A_{14}$	W14x109	W12x79	N/A	N/A	W10x12	W12x106	W10x33	W14x145	N/A
$A_{15}$	W10x22	W10x33	N/A	N/A	W10x49	W12x26	W12x65	W10x33	N/A
$A_{16}$	N/A	N/A	N/A	N/A	W10x12	N/A	W12x79	N/A	N/A
$A_{17}$	N/A	N/A	N/A	N/A	W10x33	N/A	W12x96	N/A	N/A
$A_{18}$	N/A	N/A	N/A	N/A	W12x53	N/A	W10x22	N/A	N/A
$A_{19}$	N/A	N/A	N/A	N/A	W12x72	N/A	N/A	N/A	N/A
$A_{20}$	N/A	N/A	N/A	N/A	W12x87	N/A	N/A	N/A	N/A
$A_{21}$	N/A	N/A	N/A	N/A	W12x30	N/A	N/A	N/A	N/A
<i>Shape variables (in.)</i>									
$y_1$	393	261	N/A	N/A	405	396	397	521	N/A
$y_2$	N/A	382	N/A	N/A	N/A	N/A	N/A	N/A	N/A
$y_3$	N/A	453	N/A	N/A	N/A	N/A	N/A	N/A	N/A
$y_4$	N/A	483	N/A	N/A	N/A	N/A	N/A	N/A	N/A
Weight,lb (kg)	54052.20 (24524.59)	40777.72 (18501.69)	-	-	47158.78 (21396.91)	50940.65 (23112.82)	58215.70 (26413.66)	49486.94 (22453.24)	-



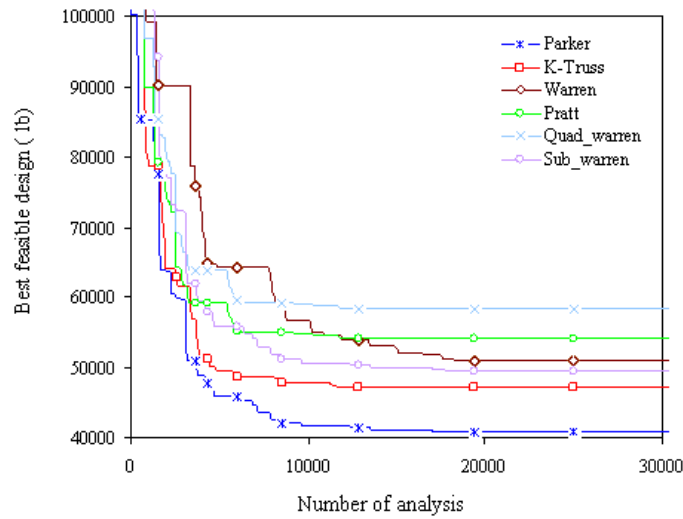
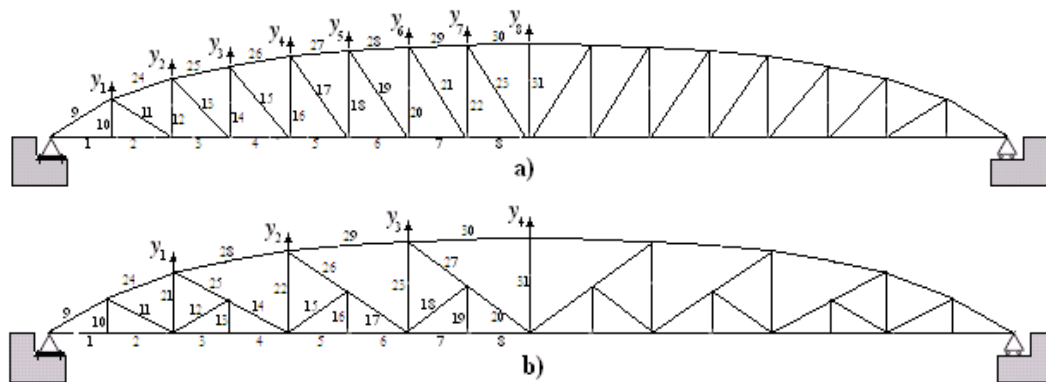


Figure 5. The design history curve of the best solution recorded under each topological form for 200ft long span bridge

4.3 Case 3: 400 ft long span bridge

In the third case study, the span length has further been increased to 400 ft. The lower chord has sixteen equal panels and it is subjected to fifteen equivalent point loads acting on each node. All the bridge topologies described formerly are applicable to this case, resulting in a total of nine candidate bridge models, seven of which have straight upper chord and the two varying height.

As the span length and accordingly the number of members increase, bridge models have nearly twice size variables compared to the previous case study: 31 size variables for Pratt, Parker, Baltimore, Petit, Warren and Subdivided Warren; 45 size variables for K- truss; 38 size variables for Quadrangular Warren; and finally 36 size variables for Whipple truss. The optimum shape of Parker and Petit forms are sought using 8 and 4 shape design variables, respectively and a single variable is used for other models. The member grouping for each model is displayed in Figure 6.



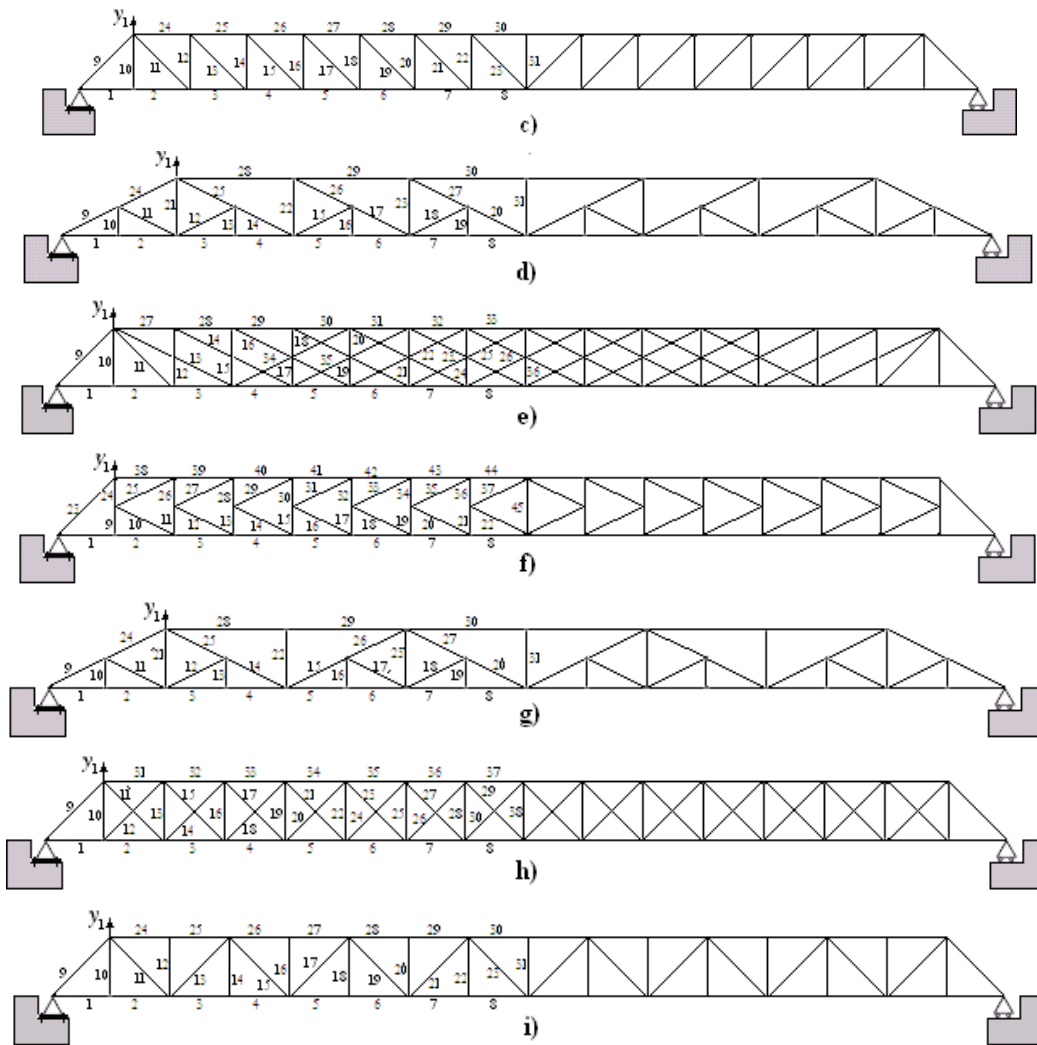


Figure 6. The topological forms used to configure 400 ft long span bridge: a) Parker, b) Petit, c) Pratt, d) Baltimore, e) Whipple, f) K-truss, g) Subdivided Warren, h) Quadrangular Warren, i) Warren

The solution algorithm is run five times independently for each bridge model and the best design yielding the least design weight is recorded. The results are tabulated in Table 3. It is clear from this table that amongst all bridge topological forms, the ones whose upper chord nodes have varying height, produce the most economical designs. The lightest bridge for 400ft long span is obtained by Petit form with a weight of 222,933.84 lb (101,149.66 kg). This design is followed by Parker form with a design weight of 225,461.20 lb (102,296.37 kg). The most uneconomical solution is 398,001.69 lb (180,581.53 kg) obtained with Pratt model. The weight difference between the lightest and heaviest designs appear to be 175,067.85 lb (79,431.87 kg), implying that a 44% saving in material is achieved with the lightest design. The design history curve is plotted in Figure 7 for each bridge model.

Table 3: Optimum designs obtained for 400ft long span bridge under various topological forms

Variable	Bridge topological forms								
	Pratt	Parker	Baltimore	Petit	K-truss	Warren	Q-Warren	S-Warren	Whipple
	<i>Size variables, ready sections</i>								
$A_1$	W12x106	W14x132	W14x61	W12x87	W10x45	W14x82	W14x82	W10x68	W12x72
$A_2$	W12x87	W12x152	W12x96	W12x87	W14x48	W12x87	W14x99	W14x176	W12x79
$A_3$	W14x120	W14x176	W12x79	W10x88	W14x82	W12x279	W12x190	W12x79	W14x120
$A_4$	W12x230	W14x193	W10x77	W10x88	W14x132	W12x230	W14x257	W14x61	W14x233
$A_5$	W14x311	W12x210	W14x145	W12x96	W14x159	W12x279	W14x283	W12x210	W14x342
$A_6$	W14x342	W14x176	W14x145	W12x96	W14x193	W12x305	W14x370	W14x176	W14x283
$A_7$	W14x370	W14x211	W14x176	W10x112	W14x233	W14x398	W14x398	W12x136	W14x283
$A_8$	W14x398	W12x230	W12x210	W12x106	W12x252	W12x305	W14x455	W14x193	W14x370
$A_9$	W14x283	W14x193	W14x193	W14x193	W10x22	W14x283	W14x257	W14x193	W14x257
$A_{10}$	W10x33	W10x12	W10x22	W10x19	W10x68	W10x33	W12x58	W10x22	W10x33
$A_{11}$	W14x159	W10x33	W10x49	W10x45	W12x65	W12x120	W14x82	W10x68	W12x106
$A_{12}$	W14x159	W10x33	W10x49	W10x60	W10x60	W12x72	W14x90	W10x49	W14x90
$A_{13}$	W14x176	W10x33	W10x22	W10x22	W10x49	W14x233	W10x33	W12x26	W12x65
$A_{14}$	W14x145	W10x33	W10x88	W10x33	W12x58	W10x39	W14x145	W12x79	W14x99
$A_{15}$	W14x145	W10x33	W10x49	W10x60	W10x49	W12x120	W10x49	W14x109	W12x65
$A_{16}$	W14x120	W10x33	W10x22	W12x26	W14x48	W12x58	W10x33	W14x34	W12x65
$A_{17}$	W14x99	W10x49	W10x49	W10x33	W10x39	W14x145	W14x74	W12x53	W12x65
$A_{18}$	W14x99	W10x49	W10x49	W12x65	W12x40	W10x39	W14x90	W12x87	W12x65
$A_{19}$	W12x87	W10x49	W10x26	W12x26	W10x33	W12x65	W10x33	W10x22	W10x33
$A_{20}$	W12x79	W10x49	W12x40	W10x33	W10x33	W12x65	W14x90	W12x53	W12x96
$A_{21}$	W14x74	W10x49	W10x49	W10x33	W10x22	W14x90	W10x49	W10x54	W10x33
$A_{22}$	W12x65	W10x49	W14x145	W10x49	W10x33	W12x45	W10x33	W12x53	W12x65
$A_{23}$	W10x49	W12x65	W14x90	W12x65	W14x370	W10x49	W12x53	W10x54	W12x65
$A_{24}$	W12x152	W14x176	W14x193	W14x176	W10x112	W12x210	W12x72	W14x176	W12x65
$A_{25}$	W12x210	W14x176	W12x87	W10x22	W14x99	W14x193	W10x33	W12x120	W12x65
$A_{26}$	W12x305	W14x193	W10x88	W10x33	W12x53	W14x283	W12x72	W14x90	W12x65
$A_{27}$	W12x336	W12x230	W10x33	W10x33	W14x90	W14x233	W10x49	W12x45	W14x159
$A_{28}$	W14x370	W14x211	W14x283	W14x342	W10x45	W14x342	W10x33	W14x311	W12x230
$A_{29}$	W14x455	W12x279	W14x342	W14x311	W14x90	W14x283	W10x49	W14x311	W14x257
$A_{30}$	W14x455	W12x230	W14x370	W14x311	W10x45	W14x283	W12x72	W14x370	W12x252
$A_{31}$	W10x33	W10x33	W10x49	W12x65	W12x79	W12x40	W14x120	W12x53	W14x398
$A_{32}$	N/A	N/A	N/A	N/A	W10x39	N/A	W14x176	N/A	W14x500
$A_{33}$	N/A	N/A	N/A	N/A	W12x65	N/A	W14x257	N/A	W14x398
$A_{34}$	N/A	N/A	N/A	N/A	W14x30	N/A	W14x283	N/A	W14x145

Variable	Bridge topological forms								
	Pratt	Parker	Baltimore	Petit	K-truss	Warren	Q-Warren	S-Warren	Whipple
$A_{35}$	N/A	N/A	N/A	N/A	W10x49	N/A	W12x336	N/A	W14x145
$A_{36}$	N/A	N/A	N/A	N/A	W10x22	N/A	W14x398	N/A	W12x65
$A_{37}$	N/A	N/A	N/A	N/A	W10x49	N/A	W14x398	N/A	N/A
$A_{38}$	N/A	N/A	N/A	N/A	W10x60	N/A	W10x33	N/A	N/A
$A_{39}$	N/A	N/A	N/A	N/A	W14x90	N/A	N/A	N/A	N/A
$A_{40}$	N/A	N/A	N/A	N/A	W14x145	N/A	N/A	N/A	N/A
$A_{41}$	N/A	N/A	N/A	N/A	W14x176	N/A	N/A	N/A	N/A
$A_{42}$	N/A	N/A	N/A	N/A	W12x190	N/A	N/A	N/A	N/A
$A_{43}$	N/A	N/A	N/A	N/A	W14x233	N/A	N/A	N/A	N/A
$A_{44}$	N/A	N/A	N/A	N/A	W12x230	N/A	N/A	N/A	N/A
$A_{45}$	N/A	N/A	N/A	N/A	W10x49	N/A	N/A	N/A	N/A
<i>Shape variables (in.)</i>									
$y_1$	579	233	724	490	720	572	528	720	523
$y_2$	N/A	373	N/A	752	N/A	N/A	N/A	N/A	N/A
$y_3$	N/A	488	N/A	856	N/A	N/A	N/A	N/A	N/A
$y_4$	N/A	578	N/A	878	N/A	N/A	N/A	N/A	N/A
$y_5$	N/A	643	N/A	N/A	N/A	N/A	N/A	N/A	N/A
$y_6$	N/A	697	N/A	N/A	N/A	N/A	N/A	N/A	N/A
$y_7$	N/A	730	N/A	N/A	N/A	N/A	N/A	N/A	N/A
$y_8$	N/A	733	N/A	N/A	N/A	N/A	N/A	N/A	N/A
Weight, lb (kg)	398001.69 (180581.53)	225461.20 (102296.37)	267499.35 (121369.94)	222933.84 (101149.66)	269186.25 (122135.32)	343921.52 (156044.25)	359947.95 (163315.77)	270521.00 (122740.93)	396280.51 (179800.59)

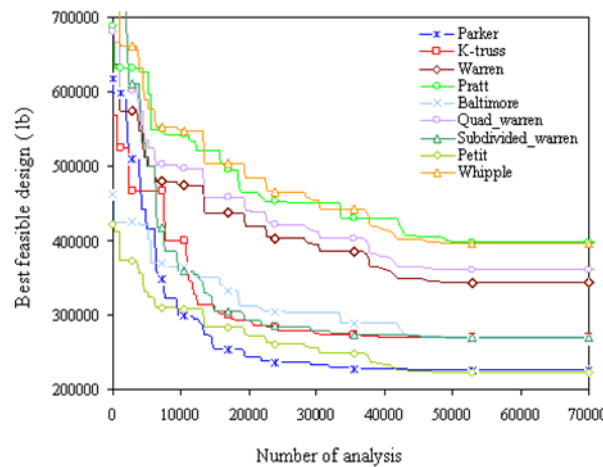


Figure 7. The design history curve of the best solution recorded under each topological form for 400ft long span bridge

#### 4.4 Case 4: 600 ft long span bridge

Finally, the span length has been increased to 600 ft in the last case study. The lower chord of the bridge consists of twenty four equal panels and it is subjected to twenty three equivalent point loads acting on each panel point. The bridge is configured according to all topological forms to generate nine competing models. Each model is then optimized for minimum weight with the cross-sectional areas of the members being the size design variables and the height of upper chord nodes being the shape design variables. The truss members are grouped considering the symmetry of the bridge around mid-span, resulting in 47 size variables for Pratt, Parker, Baltimore, Petit, Warren and Subdivided Warren, 69 for K-truss, 58 for Quadrangular Warren and 55 for Whipple truss (Figure 8). In order to determine the optimum shape of the bridge, 12 and 6 shape variables are employed for Parker and Petit trusses, respectively, whereas a single shape variable is used for other models.

Each model is separately designed five times with the SA solution algorithm implemented. The best designs obtained in these runs are tabulated in Table 4 with section designations attained for each member group and the resulting values of shape variables. The results indicate that the lightest bridge is designed with Petit form with a design weight of 624,277.4 lb (283,247.46 kg). This design is followed by Parker form, which is 722,558.3 lb (327,839.52 kg). The heaviest designs are produced by Pratt and Whipple trusses with design weights of 1,379,721.2 lb (625,841.5 kg) and 1,384,147.8 lb (627,849.4 kg), respectively. Figure 9 shows the design history curve of the best solution recorded under each topological form for 600ft long span bridge.

## 5. CONCLUSIONS

This study investigated economical design of single span truss bridge topologies under gravity loads in relation to various span length requirements. The bridges having span lengths of 100, 200, 400 and 600 ft long are first configured according to the nine topological forms (namely, Pratt, Parker, Baltimore, Petit, K-Truss, Warren, Subdivided Warren, Quadrangular Warren and Whipple), and the resulting bridge models are optimized for minimum weights using size and shape design variables together. The provisions stipulated by ASD-AISC are enforced for all the bridge models generated to ensure that the resulting structures satisfy basic strength and serviceability requirements. The minimum weight design of such structures is investigated in conjunction with the simulated annealing algorithm.

In conclusion, it is observed that the topological form chosen to generate the structural system of a bridge has a great influence on its final design weight, and consequently on its cost. The differences in design weights between the best (lightest) and worst (heaviest) models appear to be %15, 30, 43 and 55 for the span lengths of 100, 200, 400, and 600, respectively. Consequently, the selection of economical topological form becomes more pronounced and crucial as the span length of the bridge increases. This can also be observed from Figure 10, where the variation of the best design weight against the corresponding span length is plotted in Fig. 10 for each bridge topological form.

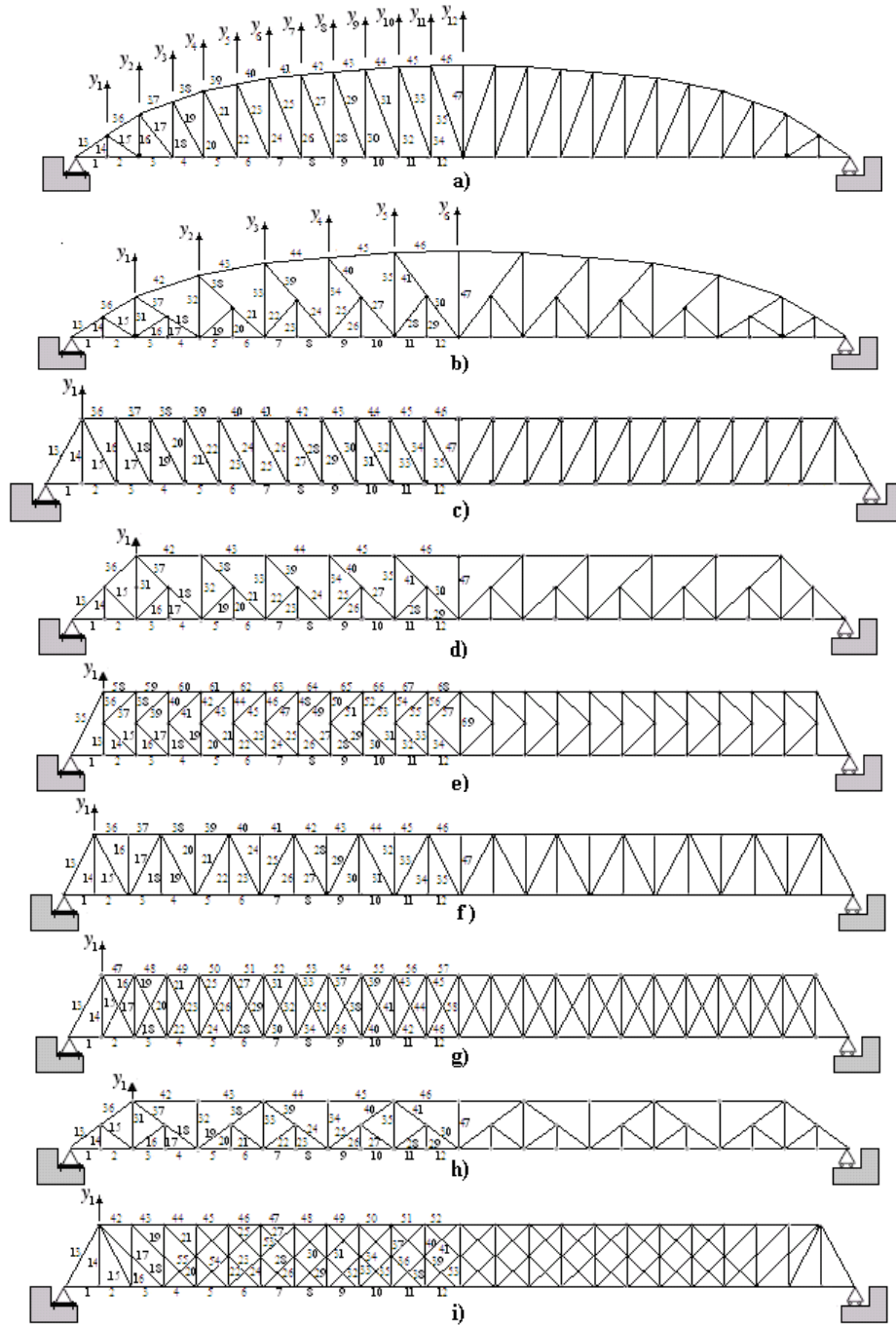


Figure 8. The topological forms used to configure 100 ft long span bridge: a) Parker, b) Petit, c) Pratt, d) Baltimore, e) K-truss, f) Warren, g) Quadrangular Warren, h) Subdivided Warren, i) Whipple

Table 4: Optimum designs obtained for 600ft long span bridge under various topological forms.

Variable	Bridge topological forms								
	Pratt	Parker	Baltimore	Petit	K-truss	Warren	Q-Warren	S-Warren	Whipple
	<i>Size variables, ready sections</i>								
$A_1$	W12x136	W14x176	W12x152	W12x152	W10x68	W14x145	W14x74	W12x190	W14x109
$A_2$	W12x79	W12x279	W12x210	W14x193	W10x77	W12x79	W12x96	W12x170	W12x152
$A_3$	W12x279	W12x230	W14x120	W14x159	W12x136	W14x455	W14x211	W12x190	W12x305
$A_4$	W14x342	W14x398	W14x145	W14x159	W12x210	W12x252	W14x311	W14x132	W14x370
$A_5$	W14x426	W12x336	W14x257	W12x170	W12x252	W14x370	W14x370	W12x336	W14x730
$A_6$	W14x605	W14x426	W12x279	W12x170	W14x342	W14x665	W14x455	W12x305	W14x730
$A_7$	W14x550	W14x455	W14x342	W12x190	W14x398	W12x279	W14x426	W12x336	W14x665
$A_8$	W14x730	W14x605	W14x370	W12x190	W14x455	W14x605	W14x605	W14x257	W14x283
$A_9$	W14x730	W14x426	W14x500	W14x211	W14x455	W14x730	W14x500	W14x426	W14x730
$A_{10}$	W14x730	W14x500	W14x730	W12x190	W14x550	W14x730	W14x730	W14x550	W14x730
$A_{11}$	W14x730	W14x500	W14x730	W14x193	W14x550	W14x605	W14x730	W14x398	W14x730
$A_{12}$	W14x730	W14x605	W14x500	W12x190	W14x550	W14x730	W14x730	W14x730	W14x730
$A_{13}$	W14x550	W14x342	W14x311	W14x311	W12x26	W14x550	W14x550	W14x342	W14x455
$A_{14}$	W12x53	W14x74	W10x26	W14x43	W12x136	W12x79	W12x53	W14x34	W10x49
$A_{15}$	W14x257	W14x132	W10x49	W10x60	W14x99	W14x233	W14x211	W10x100	W14x176
$A_{16}$	W14x426	W12x79	W10x49	W10x88	W14x120	W14x132	W14x145	W12x170	W14x176
$A_{17}$	W12x336	W12x120	W12x26	W12x35	W14x90	W14x500	W14x90	W12x65	W12x152
$A_{18}$	W14x398	W12x87	W12x210	W12x65	W10x112	W14x74	W14x342	W14x193	W14x90
$A_{19}$	W14x311	W12x65	W10x49	W12x65	W14x90	W12x252	W12x87	W14x233	W12x210
$A_{20}$	W14x370	W12x40	W12x26	W10x39	W10x112	W14x90	W12x53	W14x30	W14x90
$A_{21}$	W14x257	W10x49	W12x170	W10x45	W12x79	W14x455	W10x112	W12x87	W12x65
$A_{22}$	W14x311	W10x49	W10x54	W14x90	W10x100	W12x65	W14x211	W12x65	W10x88
$A_{23}$	W12x252	W14x74	W12x26	W10x39	W12x72	W14x159	W10x49	W12x30	W12x65
$A_{24}$	W14x257	W14x90	W12x170	W12x58	W10x100	W14x233	W14x233	W14x176	W10x49
$A_{25}$	W14x211	W12x65	W10x49	W14x109	W12x65	W14x311	W12x96	W12x190	W12x65
$A_{26}$	W14x233	W10x60	W12x26	W10x68	W14x82	W10x88	W10x49	W10x26	W10x49
$A_{27}$	W12x190	W12x65	W12x120	W14x82	W10x54	W12x120	W12x96	W10x68	W12x210
$A_{28}$	W14x193	W12x72	W10x49	W14x99	W12x79	W14x90	W14x176	W14x109	W12x65
$A_{29}$	W14x211	W12x65	W10x39	W10x54	W10x49	W14x233	W10x49	W10x39	W14x99
$A_{30}$	W14x159	W12x65	W12x40	W10x60	W10x60	W10x68	W14x176	W14x48	W12x252
$A_{31}$	W12x210	W12x72	W12x65	W12x45	W10x49	W14x176	W12x72	W12x136	W12x65
$A_{32}$	W14x120	W12x72	W14x342	W10x49	W14x48	W14x120	W10x49	W12x136	W14x90
$A_{33}$	W12x120	W14x109	W14x283	W14x99	W12x26	W14x176	W12x72	W12x87	W12x65
$A_{34}$	W14x159	W12x65	W14x193	W14x90	W10x33	W12x65	W14x145	W14x211	W14x455
$A_{35}$	W12x96	W14x90	W14x176	W14x145	W14x665	W14x120	W12x53	W12x120	W10x49
$A_{36}$	W12x305	W14x342	W14x283	W14x283	W12x230	W14x283	W14x145	W14x283	W12x65
$A_{37}$	W14x283	W14x370	W12x210	W12x45	W14x159	W12x190	W12x65	W14x145	W14x455
$A_{38}$	W14x370	W14x550	W12x252	W10x77	W14x109	W14x398	W10x49	W12x279	W10x49
$A_{39}$	W14x730	W14x426	W14x145	W10x33	W14x109	W14x342	W12x65	W14x193	W14x109
$A_{40}$	W14x730	W14x426	W14x109	W12x58	W14x109	W14x730	W14x145	W14x193	W12x65
$A_{41}$	W14x730	W14x455	W10x88	W10x54	W14x145	W14x500	W10x49	W12x136	W12x65
$A_{42}$	W14x730	W14x455	W14x398	W14x550	W12x96	W14x730	W14x145	W14x426	W14x370

Variable	Bridge topological forms								
	Pratt	Parker	Baltimore	Petit	K-truss	Warren	Q-Warren	S-Warren	Whipple
$A_{43}$	W14x730	W14x398	W14x550	W14x550	W14x132	W14x605	W12x72	W14x398	W14x550
$A_{44}$	W14x730	W14x550	W14x605	W14x500	W10x88	W14x730	W10x49	W14x730	W14x550
$A_{45}$	W14x730	W14x605	W14x665	W14x500	W14x109	W14x730	W12x65	W14x605	W14x500
$A_{46}$	W14x730	W14x550	W14x730	W14x500	W10x88	W14x730	W14x145	W14x730	W14x550
$A_{47}$	W10x49	W12x65	W12x65	W14x176	W14x99	W10x100	W14x145	W12x72	W14x730
$A_{48}$	N/A	N/A	N/A	N/A	W12x72	N/A	W12x210	N/A	W14x730
$A_{49}$	N/A	N/A	N/A	N/A	W14x99	N/A	W14x311	N/A	W14x730
$A_{50}$	N/A	N/A	N/A	N/A	W10x68	N/A	W14x426	N/A	W14x730
$A_{51}$	N/A	N/A	N/A	N/A	W12x87	N/A	W14x398	N/A	W14x730
$A_{52}$	N/A	N/A	N/A	N/A	W12x53	N/A	W14x665	N/A	W14x730
$A_{53}$	N/A	N/A	N/A	N/A	W12x65	N/A	W14x550	N/A	W14x455
$A_{54}$	N/A	N/A	N/A	N/A	W12x53	N/A	W14x730	N/A	W14x455
$A_{55}$	N/A	N/A	N/A	N/A	W12x65	N/A	W14x730	N/A	W14x455
$A_{56}$	N/A	N/A	N/A	N/A	W12x40	N/A	W14x730	N/A	N/A
$A_{57}$	N/A	N/A	N/A	N/A	W12x65	N/A	W14x730	N/A	N/A
$A_{58}$	N/A	N/A	N/A	N/A	W12x79	N/A	W12x53	N/A	N/A
$A_{59}$	N/A	N/A	N/A	N/A	W12x152	N/A	N/A	N/A	N/A
$A_{60}$	N/A	N/A	N/A	N/A	W14x211	N/A	N/A	N/A	N/A
$A_{61}$	N/A	N/A	N/A	N/A	W14x283	N/A	N/A	N/A	N/A
$A_{62}$	N/A	N/A	N/A	N/A	W14x342	N/A	N/A	N/A	N/A
$A_{63}$	N/A	N/A	N/A	N/A	W14x398	N/A	N/A	N/A	N/A
$A_{64}$	N/A	N/A	N/A	N/A	W14x455	N/A	N/A	N/A	N/A
$A_{65}$	N/A	N/A	N/A	N/A	W14x500	N/A	N/A	N/A	N/A
$A_{66}$	N/A	N/A	N/A	N/A	W14x550	N/A	N/A	N/A	N/A
$A_{67}$	N/A	N/A	N/A	N/A	W14x550	N/A	N/A	N/A	N/A
$A_{68}$	N/A	N/A	N/A	N/A	W14x665	N/A	N/A	N/A	N/A
$A_{69}$	N/A	N/A	N/A	N/A	W12x65	N/A	N/A	N/A	N/A
	<i>Shape variables (in.)</i>								
$y_1$	739	222	802	450	867	726	733	810	638
$y_2$	N/A	363	N/A	736	N/A	N/A	N/A	N/A	N/A
$y_3$	N/A	445	N/A	956	N/A	N/A	N/A	N/A	N/A
$y_4$	N/A	549	N/A	1110	N/A	N/A	N/A	N/A	N/A
$y_5$	N/A	640	N/A	1157	N/A	N/A	N/A	N/A	N/A
$y_6$	N/A	704	N/A	1167	N/A	N/A	N/A	N/A	N/A
$y_7$	N/A	769	N/A	N/A	N/A	N/A	N/A	N/A	N/A
$y_8$	N/A	817	N/A	N/A	N/A	N/A	N/A	N/A	N/A
$y_9$	N/A	860	N/A	N/A	N/A	N/A	N/A	N/A	N/A
$y_{10}$	N/A	887	N/A	N/A	N/A	N/A	N/A	N/A	N/A
$y_{11}$	N/A	895	N/A	N/A	N/A	N/A	N/A	N/A	N/A
$y_{12}$	N/A	900	N/A	N/A	N/A	N/A	N/A	N/A	N/A
Weight,lb (kg)	1379721.2 (626007.80)	722558.3 (327839.52)	869646.4 (394576.41)	624277.4 (283247.46)	830048.1 (376609.85)	1150368.2 (521945.64)	1090091.5 (494596.87)	855874.5 (388327.81)	1384147.8 (628016.24)



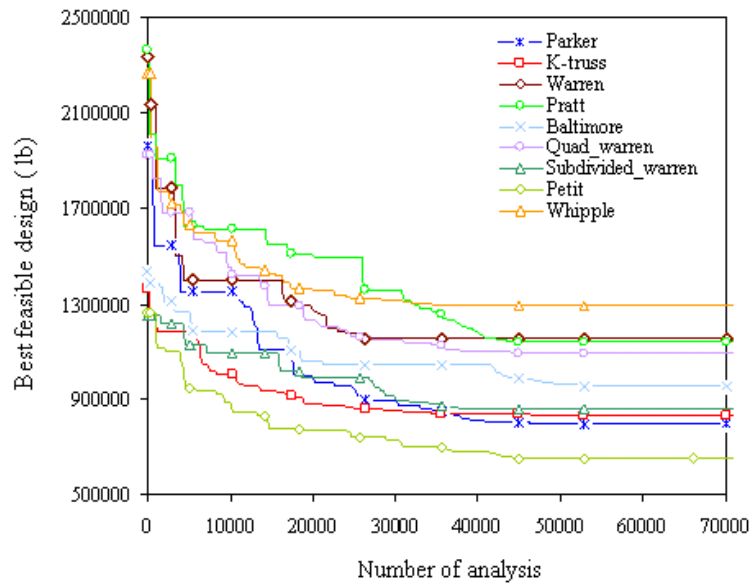


Figure 9. The design history curve of the best solution recorded under each topological form for 600ft long span bridge

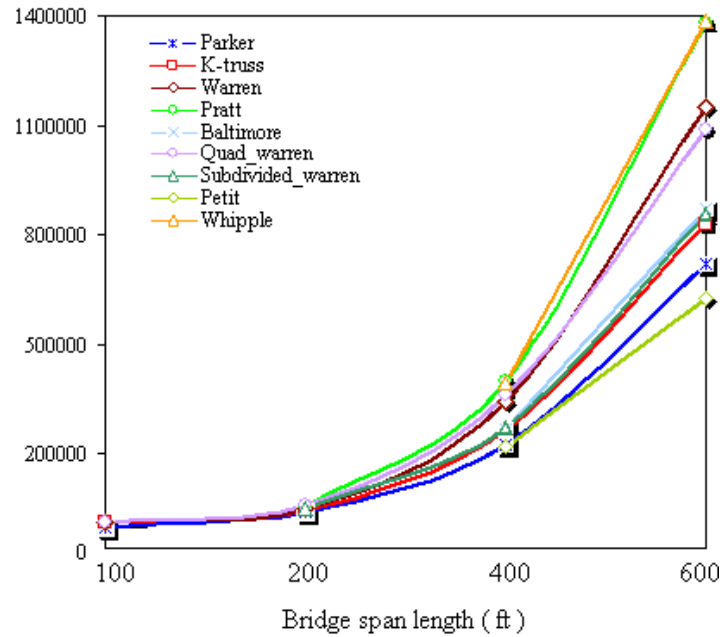


Figure 10. A comparison of design weights obtained with various topological forms for 100, 200, 400 and 600 ft long span bridges

Petit and Parker trusses, which have polygonal upper chords seem to be the most weight-effective models since they yield the minimum design weights in all case studies considered.

The resulting optimum shapes of the bridge developed with Petit and Parker trusses are such that bridge height is reduced from mid-span towards the ends to eliminate unnecessary material use in the design. This can be verified by an analogy to the behaviour of a simply supported beam subjected to distributed transverse loading, where the bending moment is maximum at mid-span and goes towards zero when approaching the ends. These two models can economically be used for all span length requirements.

The results also indicate that some bridge forms, such as Whipple and Pratt should be avoided for all span lengths, and Warran and Quadrangular Warren for relatively long span lengths as far as the weight efficiency of the resulting bridge is concerned. Baltimore, Subdivided Warran and K-truss form lead to design weights in some similar scales. These forms benefit from reducing member lengths and thus increasing significantly out-of-plane buckling strengths of the members.

## REFERENCES

1. *Manual of Steel Construction, Allowable Stress Design*, 9<sup>th</sup> edition, AISC, American Institutes of Steel Construction, Inc, Chicago, Illinois, USA, 1989.
2. Hasançebi O. Adaptive evolution strategies in structural optimization: enhancing their computational performance with applications to large-scale structures, *Computers and Structures*, **86** (2008) 119-32.
3. Bennage WA, and Dhingra AK. Single and multi-objective structural optimization in discrete-continuous variables using simulated annealing, *International Journal in Numerical Methods in Engineering*, **38** (1995) 2753–73.
4. Hasançebi O, Çarbaş S, Doğan E, Erdal F, and Saka, MP. Performance evaluation of metaheuristic search techniques in the optimum design of real size pin jointed structures. *Computers and Structures*, **87** (2009) 284-302.
5. Kirkpatrick S, Gelatt CD, and Vecchi MP. Optimization by simulated annealing, *Science*, **220**(1983) 671–80.
6. Shim PY, and Manoochehri S. Generating optimal configurations in structural design using simulated annealing, *International Journal for Numerical Methods in Engineering*, **40**(1997) 1053–69.
7. Ceramic B, Fryer C, and Baires RW. An application of simulated annealing to the optimum design of reinforced concrete retaining structures, *Computers and Structures*, **79**(2001) 1569–81.
8. Hasançebi O, and Erbatur F. Layout optimisation of trusses using simulated annealing, *Advances in Engineering Software*, **33**(2002) 681–96.
9. Değertekin SÖ. A comparison of simulated annealing and genetic algorithm for optimum design of nonlinear steel space frames, *Structural and Multidisciplinary Optimization*, **34**(2007) 347–59.
10. Hasançebi O, Çarbaş S, and Saka MP. Improving the performance of simulated annealing in structural optimization, *Structural and Multidisciplinary Optimization*, **41**(2010) 189–203.
11. ASCE 7-05, Minimum Design Loads for Building and Other Structures, 2005.